Inorganic Chemistry

Article

pubs.acs.org/IC

Pyrazine Motif Containing Hexagonal Macrocycles: Synthesis, Characterization, and Host–Guest Chemistry with Nitro Aromatics

Sourav Bhowmick,[†] Sourav Chakraborty,[†] Atanu Das,[‡] Sivaramaiah Nallapeta,[§] and Neeladri Das*[,†]

[†]Department of Chemistry, Indian Institute of Technology Patna, Patna 800 013, Bihar, India

[‡]Department of Chemistry, University of Texas at Austin, Austin, Texas 78712, United States

[§]Bruker Daltonics India, Bruker Centre of Excellence, Bangalore-560092, India

Supporting Information

ABSTRACT: The synthesis and characterization of cationic two-dimensional metallamacrocycles having a hexagonal shape and cavity are described. Both macrocycles utilize a pyrazine motif containing an organometallic acceptor tecton with platinum(II) centers along with different donor ligands. While one macrocycle is a relatively larger [6 + 6], the other is a relatively smaller [2 + 2] polygon. A unique feature of the smaller ensemble is that it is an irregular polygon in which all six edges are not of equal length. Molecular modeling of these macrocycles confirmed the presence of hexagonal cavities. The ability of these π-electron rich macrocycles to act as potential hosts for relatively electron deficient nitroaromatics (DNT = 2,4-dinitrotoluene and PA = picric acid) has been studied using isothermal titration calorimetry (ITC) as a tool. Molecular dynamics simulation studies were subsequently performed to gain critical insight into the binding interactions between the nitroaromatic guest molecules (PA/DNT) and the ionic macrocycles reported herein.

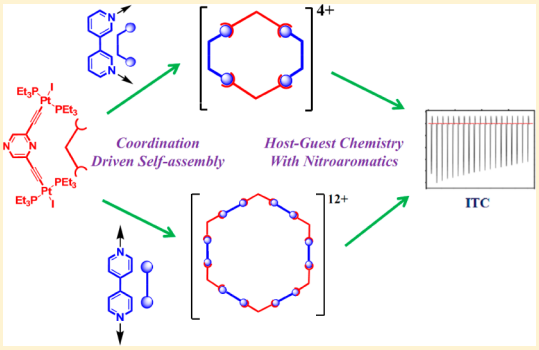

INTRODUCTION

The use of coordination bonds in the synthesis of discrete nanoscalar frameworks is presently a popular research area among contemporary supramolecular chemists.[1] This is reflected in the increase in number of reports and reviews describing construction of metallasupramolecular structures using "coordination driven self assembly" protocol in the past few years.[2] Using this methodology that relies on metal–ligand interactions, various two-dimensional polygons and three-dimensional polyhedra have been constructed.[1−3] Several supramolecules have also emerged as functional materials with application in fields including but not limited to host–guest chemistry (molecular recognition), catalysis, and sensing.[4]

As far as the two-dimensional metallamacrocycles are concerned, the "coordination driven self assembly" approach has yielded molecular polygons of various shapes and sizes.[1a,b,5] In this context, it must be mentioned that there are relatively lesser examples of higher polygons (molecular pentagons, hexagons, etc.) than smaller ring systems (molecular triangles, rhomboids, squares, and rectangles).[6] This is because the design of larger ring systems usually requires association of a larger number of tectons (building blocks), and hence synthesis of these two-dimensional ensembles is more challenging.

Among the higher order two-dimensional polygons, the hexagonal motifs are encountered more often in nature. This geometrical shape has often been referred to as nature's "perfect shape" and examples in nature which incorporate this structural motif include but are not limited to the beehive honeycomb, scutes of a turtle's carapace, snowflakes, and graphite. This shape has also been recognized by human beings as the one of the most efficient shapes. This explains why, in engineering, nuts and bolt heads are hexagonal.

The predominance of this shape may have fueled interest among chemists to design hexagonal metallamacrocycles with six edges.[7] The directional bonding protocol systematized by Stang and co-workers dictates that macrocycles with six sides can be constructed by two different synthetic strategies. The first approach is based on the reaction of two types of complementary ditopic tectons, each having 120° angles between the reactive sites.[8] The second approach requires combination of six units of an angular building block possessing a turning angle of 120° with six units of complementary linear ones having a 180° bite angle.[9]

In the field of coordination driven supramolecular chemistry, organometallic complexes with platinum(II) centers have emerged as one of the most popular choices for acceptor tectons.[10] Recently, we have reported the synthesis of a new pyrazine based ditopic organometallic complex containing platinum ethynyl motifs.[11] It was further shown that this acceptor tecton can act as a host for compounds present in nitroaromatic explosives.

Herein, we report application of this pyrazine based 120° Pt^{II}_2-organometallic complex as a synthon for the construction

Received: May 22, 2015
Published: September 11, 2015

DOI: 10.1021/acs.inorgchem.5b01156
Inorg. Chem. 2015, 54, 8994−9001

of cationic molecular polygons that have a hexagonal shape. The macrocycles reported herein are unique examples of pyrazine motif containing cationic metallasupramolecular polygons. These newly synthesized macrocycles were completely characterized by multinuclear NMR spectroscopy including ^{1}H DOSY, ESI-TOF mass spectrometry and elemental analyses techniques. Further insight into the shape and size of these ionic macrocycles was obtained via molecular simulation, employing the PM6 semiempirical molecular orbital method. The resulting macrocycles are e-rich due to the presence of platinum ethynyl motifs. In this context, it must be mentioned that molecular ensembles containing Pt-ethynyl motifs have found potential application in the efficient detection of electron deficient nitroaromatic explosive materials in trace quantities.[4e] The fact that the macrocycles reported herein have several platinum ethynyl units in their backbone has been further exploited to study their host−guest interactions with nitroaromatics (DNT = 2,4-dinitrotoluene and PA = picric acid). Isothermal titration calorimetry has been used as an analytical tool to show host−guest complex formation between these macrocycles and nitroaromatic guest molecules. Results obtained from calorimetric titration experiments were supported by theoretical computational simulation studies.

RESULTS AND DISCUSSION

According to the "directional bonding approach," the prerequisite required for the design of a convex supramolecular polygon framework is the availability of at least two complementary building blocks (tectons), each having two divergent reactive sites present in them. The knowledge of the angular separation (θ) between the two reactive binding sites (in case of each tecton) is important for predicting the shape of the anticipated two-dimensional ensemble.[1b,l] In the specific case of a molecular hexagon, two kinds of frameworks are reported in the literature. In the first type, one of the building blocks occupies the vertices of the polygon and the other complementary building block defines the edges of the polygon (Chart 1a). This is possible because, in these polygons, the former building block is angular with a turning angle (θ) of 120° while the complementary tecton is linear having bite angle (θ) equal to 180°. The synthesis of this type of framework requires the assembly of twelve [6 + 6] tectons. In case of the second type of discrete hexagonal molecular polygons reported in the literature, both complementary building blocks (tectons) occupy the vertices of the molecular hexagon (Chart 1b). Since a hexagon has six vertices and two complementary tectons are used, the construction of this latter type of "trimeric" hexagon requires self-assembly of six [3 + 3] tectons and is therefore relatively less complex than the former "hexameic" ensembles. We propose a third strategy for the design of discrete hexagonal polygons that utilizes fewer building blocks. In this methodology, if one of the tectons occupies two vertices, then reaction with a complementary angular tecton (with a turning angle of 120°) will yield a finite hexagon via a [2 + 2] self-assembly process (Chart 1c). 3,3′-Bipyridine can be considered as a ditopic donor tecton that can yield such kinds of a "dimeric" molecular hexagon via a much simpler [2 + 2] assembly of appropriate tectons.

Chart 1. Cartoon Representation of (a) [6 + 6], (b) [3 + 3], and (c) [2 + 2] Hexagons

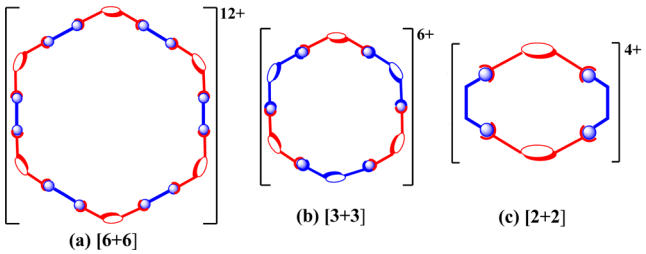

It must be mentioned here that in case of the aforementioned "hexameric" and "trimeric" frameworks (a and b in Chart 1), the resulting polygons are convex and regular. These are convex because the magnitude of each of the six interior angles is less than 180°. Additionally, each side of these resulting polygons (a and b in Chart 1) is of the same length, and all interior angles are congruent (120°). Therefore, these polygons are regular because, by definition, regular polygons have congruent sides (equilateral) and congruent interior angles (equiangular). In case of the third structure (c in Chart 1), the resulting macrocycle is also a convex hexagon. Here, every interior angle measures 120°. However, the building blocks defining the six sides of this polygon are not the same. As a result, all sides of this polygon (c in Chart 1) are not congruent, and hence it (c in Chart 1) is irregular (equiangular but not equilateral).

To illustrate this point, self-assembly and characterization of two cationic hexagons (a regular and another non regular) employing a pyrazine based ditopic acceptor tecton is being described herein (Scheme 1).

Self-assembly and Characterization of Molecular Hexagons. The diplatinum acceptor tecton (**1**) was first reacted with two equivalents of silver nitrate and subsequently with an appropriate ditopic donor tecton (3,3′-bipyridine or 4,4′-bipyridine) in a 1:1 stoichiometric ratio. This resulted in the exclusive formation of the desired ionic molecular hexagon **2** and **3** via [2 + 2] and [6 + 6] coordination driven self-assembly, respectively. After evaporation of the solvent under reduced pressure, the crude product thus obtained was washed with diethyl ether and subsequently recrystallized from methanol to obtain the desired macrocycles as a yellowish microcrystalline solid in high yields (>80%). In both cases, the product exhibited high solubility in common organic solvents. The newly prepared self-assembled compounds were subsequently characterized by using multinuclear NMR spectroscopy, mass spectrometry (ESI-TOF-MS), and elemental analyses. In each case, the formation of a single discrete molecular ensemble was initially evident from their respective ^{31}P{^{1}H} and ^{1}H spectral analyses. The appearance of a sharp singlet (δ 15.25 ppm for **2** and 15.78 ppm for **3**) in the respective ^{31}P{^{1}H} NMR spectrum (Figure 1a and Supporting Information S3) along with an associated pair of platinum satellite peaks (**2**, $^1J_{PPt}$ = 1131 Hz; **3**, $^1J_{PPt}$ = 1135 Hz) clearly reflected the formation of single highly symmetrical species in which all phosphorus nuclei are chemically equivalent. In addition, the significant downfield shifts of the phosphorus peaks in products (**2** and **3**) relative to **1** indicate incorporation of a newer metal−ligand coordination bond around the Pt centers due to cleavage of Pt−I bonds in **1**. The ^{1}H NMR spectra of **2** and **3** also suggested the incorporation of a donor tecton (3,3′-bipyridine in case of **2** or 4,4′-bipyridine in case of **3**) and acceptor pyrazine based tecton (**1**) in the respective final product. A representative proton NMR spectrum of **2** is shown in Figure 1b. Here the signals at 9.04, 8.87, 8.56, and

DOI: 10.1021/acs.inorgchem.5b01156
Inorg. Chem. 2015, 54, 8994−9001

Scheme 1. Design of Macrocycles 2 and 3

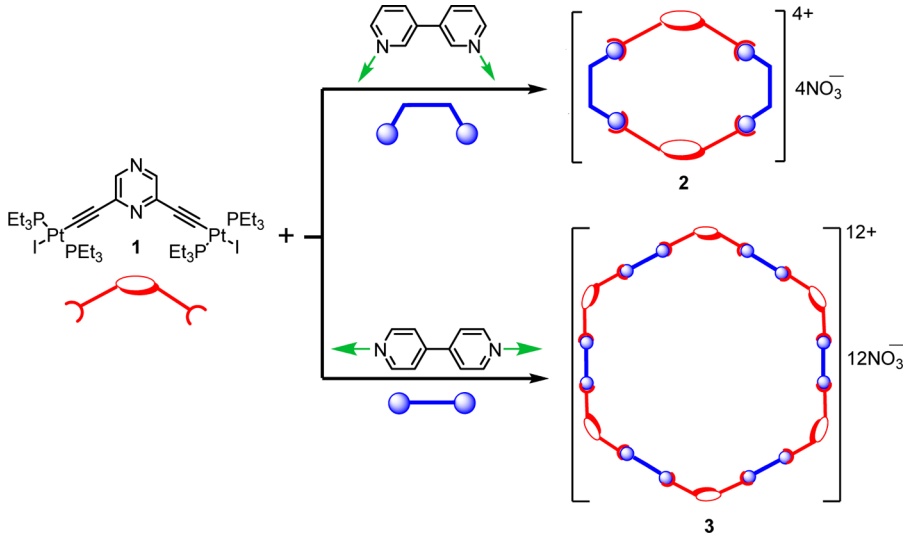

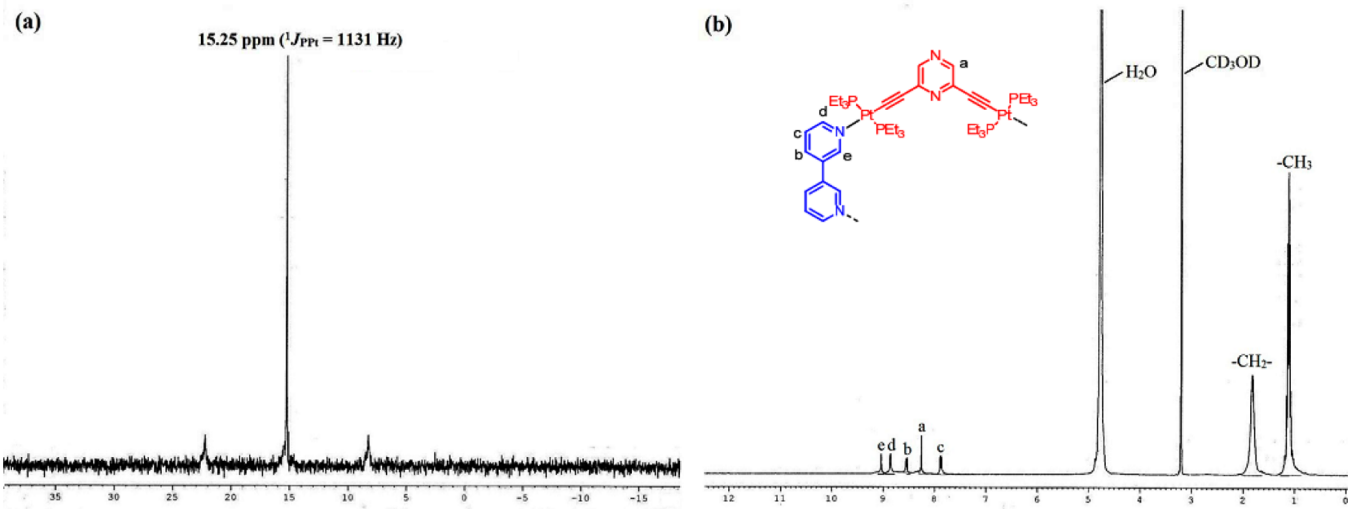

Figure 1. (a) $^{31}P\{^{1}H\}$ and (b) ^{1}H NMR spectra of macrocycle **2**.

7.90 ppm correspond to the protons of 3,3′-bipy moieties. A sharp singlet at 8.26 ppm corresponds to the protons of the pyrazine moiety. The ethyl protons of the phosphine moiety attached to platinum centers are observed in the range 1.88−1.08 ppm. Similarly, in the case of **3**, all proton signals in ^{1}H NMR were assigned precisely (Supporting Information S3). In the case of both products (**2** and **3**), the integration of the proton NMR signals due to bipyridine bridging ligands and pyrazine based Pt^{II}_2 units suggest a self-assembly of these building blocks in a 1:1 stoichiometric ratio. The purity of these self-assembled products (**2** and **3**) was further ratified from their respective ^{1}H DOSY NMR spectrum, wherein the appearance of a single trace confirmed the formation of a single product and simultaneously ruled out the possibility of the presence of impurities in the form of other macrocycles or oligomeric byproduct(s) in solution (Supporting Information S4).

The actual composition of **2** and **3** was ascertained by mass spectrometric (ESI-TOF-MS) analyses (Supporting Information S4,S5). In the case of compound **2**, its ESI-TOF-MS spectrum (Figure 2) showed peaks at m/z = 2474.73 $[\mathbf{2}\text{-}NO_3]^{+}$, 1206.37 $[\mathbf{2}\text{-}2NO_3]^{2+}$, 783.58 $[\mathbf{2}\text{-}3NO_3]^{3+}$, and 572.19 $[\mathbf{2}\text{-}4NO_3]^{4+}$ which are attributed to the consecutive loss of nitrate counteranions assuming the formation of the M_2L_2 macrocycle [M = Pt^{II}_2 acceptor **1**, L = 3,3′-bipy]. Similarly for compound **3**, the corresponding ESI-TOF-MS spectrum (Figure 2) exhibited signals at m/z = 1840.55 $[\mathbf{3}\text{-}4NO_3]^{4+}$, 1206.37 $[\mathbf{3}\text{-}6NO_3]^{6+}$, 889.28 $[\mathbf{3}\text{-}8NO_3]^{8+}$, 783.58 $[\mathbf{3}\text{-}9NO_3]^{9+}$, 629.84 $[\mathbf{3}\text{-}11NO_3]^{11+}$, and 572.19 $[\mathbf{3}\text{-}12NO_3]^{12+}$ corresponding to the formation of M_6L_6 species [M = Pt^{II}_2 acceptor **1**, L = 4,4′-bipy]. Thus, mass spectrometry was used as a useful analytical tool to unambiguously confirm that the self-assembly reaction of the pyrazine based 120°-Pt^{II}_2 acceptor linker (**1**) with angular 3,3′-bpy leads to the formation of a [2 + 2] ionic metallamacrocycle, while the reaction of **1** and linear ditopic 4,4′-bpy donor ligands results in the formation of [6 + 6] discrete and cationic supramolecular frameworks.

All attempts to grow single crystals of these self-assembled metallacycles (**2** and **3**) for structural characterization have proven unsuccessful to date. Under these circumstances, structural information on these metallacycles was obtained by optimizing their respective geometry utilizing the PM6 semiempirical molecular orbital method.[12] The energy minimized structure for both self-assembled macrocyclic

DOI: 10.1021/acs.inorgchem.5b01156
Inorg. Chem. 2015, 54, 8994−9001

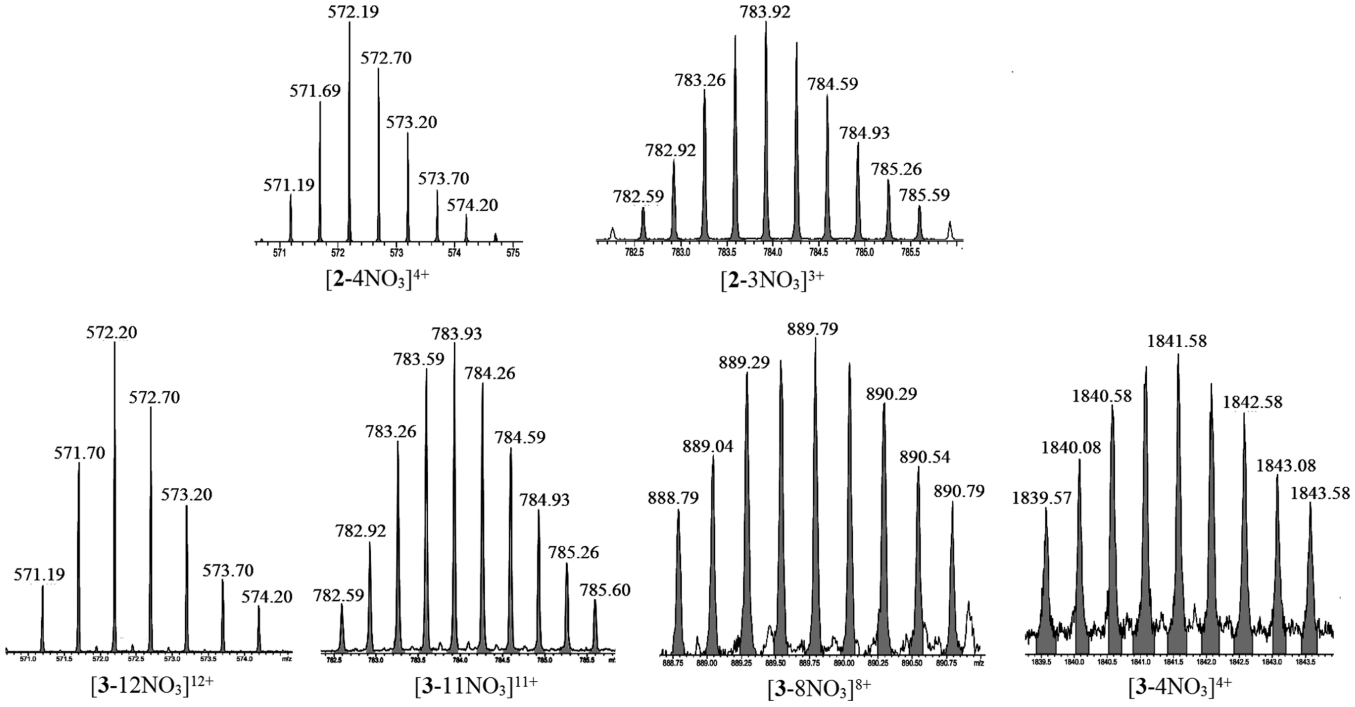

Figure 2. Selected charge states for macrocycles **2** and **3** observed by ESI-TOF-MS spectrometry.

products (**2** and **3**) was largely planar and hexagonal in shape (Figure 3). The presence of a hexagonal cavity is also clearly

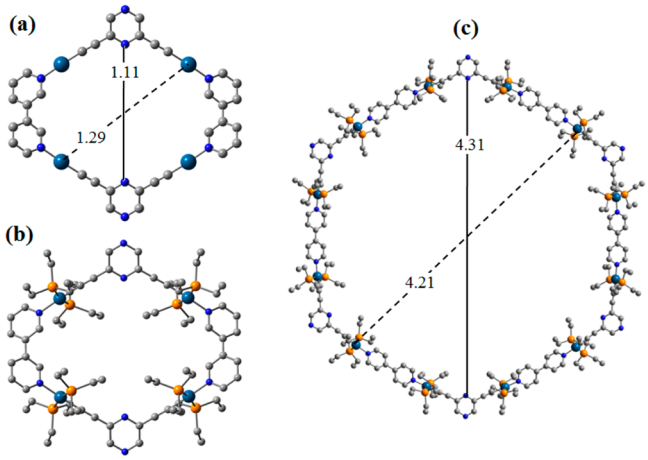

Figure 3. Simulated ball and stick molecular model optimized by PM6 semiempirical molecular orbital methods: (a and b) macrocycle **2** (phosphine ligands are omitted in a), (c) macrocycle **3**. Color code: light gray, C; orange, P; dark cyan, Pt; blue, N. H atoms are omitted for clarity. Unit of distances measured is nanometers.

evident from the space filling model of these macrocycles (Supporting Information S5). This is in line with the prediction that one can make based on the tenets of the "Directional Bonding Approach" as outlined in Chart 1. In the case of self-assembled product **2**, two units each of 3,3′-bipy (donor) and pyrazine based organometallic (acceptor) tectons combine to yield a convex hexagon that is irregular (all sides are not of equal length) albeit equiangular. In this well-defined hexagonal supramolecular macrocycle, the length of the two edges is 0.43 nm, while the length of the other four edges is 0.93 nm. On the other hand, in the case of a [6 + 6] self-assembled ensemble involving 4,4′-bipy (donor), the resulting hexagon is a regular polygon, with each side measuring 2.3 nm. The distance between two diagonally opposite endocyclic nitrogens of pyrazine moieties was found to be 1.11 nm for [2 + 2] macrocycle **2**, while in case of the [6 + 6] hexameric macrocycle (**3**), the distance is relatively larger and estimated to be 4.31 nm. The average distance between two opposite Pt atoms was measured to be 1.29 and 4.21 nm for hexagons **2** and **3**, respectively (Figure 3). Optimized geometry also indicated that in both cases (**2** and **3**), there was a slight distortion from a square planar geometry at the platinum centers.

Study of Host–Guest Complexation between Macrocyclic Host (2 and 3) and Nitroaromatic Guests Using Calorimetric Titration. Compounds **2** and **3** have the following two characteristics. First, these have multiple Pt-ethynyl linkages in the polygon backbone that renders them π-electron-rich species relative to nitroaromatic compounds that are relatively electron deficient species due to the presence of one or more e-withdrawing nitro functional groups. Second, the hexagonal self-assembled ensembles are convex polygons and hence have a spacious internal cavity for exhibiting encapsulation chemistry with a guest of suitable size. Therefore, we were interested to explore host–guest interactions of these cationic pyrazine motif containing metallamacrocycles with nitroaromatics such as picric acid (PA) and 2,4-dinitrotoluene (DNT).

Usually, it is reported in the literature that the presence of Pt-ethynyl motifs renders the molecule fluorescent in nature, and hence fluorescence (quenching) spectroscopy is used as a tool for studying their host–guest interactions with electron poor quenchers.[4e,10a,b] We have previously reported that the organometallic acceptor linker (**1**) is nonfluorescent in nature.[11] Hence, in the present case, ensembles **2** and **3** derived from **1** are nonfluorescent in nature. This limits, herein, the use of fluorescence spectroscopy as an analytical tool to study host–guest complexation between these electron-rich

DOI: 10.1021/acs.inorgchem.5b01156
Inorg. Chem. 2015, 54, 8994–9001

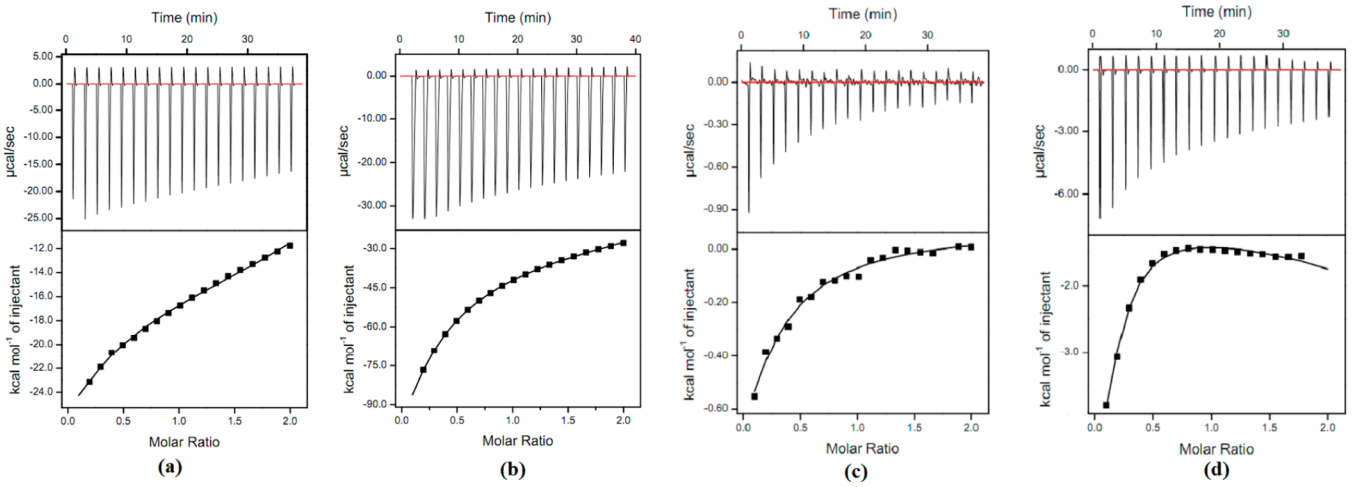

Figure 4. ITC isotherm (above) and ITC data points best fitted with a sequential three-site binding model (below) for the titration of macrocycles (5 mM) into nitroaromatics (0.5 mM) at 298 K in methanol. (a) Macrocycle **2** with PA, (b) macrocycle **3** with PA, (c) macrocycle **2** with DNT, and (d) macrocycle **3** with DNT.

frameworks (**2** and **3**) and relatively electron deficient nitroaromatics. Under these circumstances, isothermal titration calorimetry (ITC) was appropriately used to study the above-mentioned host–guest chemistry.

In contemporary research, ITC has emerged as a powerful analytical tool for studying molecular recognition between supramolecular host and guest species.[13] The magnitude of binding interactions and other thermodynamic parameters can be estimated precisely using this calorimetry technique.

The ITC titrations between macrocylic hosts (**2** or **3**) and selected nitroaromatic guests (picric acid or 2,4-DNT) were recorded at 25 °C and are shown in Figure 4. The ITC traces suggest that, in these studies, the binding interactions are exothermic in nature. In the case of complexation between PA and either macrocycles (**2** or **3**), the ITC data points were found to fit best with a three-sites sequential binding model, and the data did not fit satisfactorily with other binding models. The thermodynamic parameters as obtained by ITC data are tabulated in Table S1 (Supporting Information). The binding constants as obtained from calorimetric titration were found to be on the order of order 10^4 to 10^5 M^{-1} (Table S1), which suggests very strong binding interactions between PA and the macrocycles **2** and **3**. The ITC data also clearly indicated that, for either macrocycle (**2** or **3**) and picric acid, the difference in the magnitude of binding free energy between three binding sites is nominal (~0.1–0.2 kcal/mol). Similarly, in the case of host–guest complexation between metallamacrocycles (**2** or **3**) and DNT, thr best fit of ITC data points corresponds to the three sites sequential binding model. In general, the magnitude of the binding constants as obtained from the ITC experiments (Table S1) suggests that pyrazine containing macrocycles have relatively higher binding affinity for picric acid than DNT molecules as a guest moiety.

Theoretical Calculation. Molecular dynamics simulation studies were performed to have a critical insight into the binding interactions between the nitroaromatics (PA/DNT) and the pyrazine based ionic macrocycles **2** and **3**. It has been shown from ITC experimental data that the macrocycle **2** and **3** have three binding sites for the nitroaromatic guests. To generate the equilibrium ensemble of the nitroaromatic bound macrocycles, both the nitroaromatic compounds were put in the center of each of the macrocycles separately, leading to four different macrocycle–nitroaromatic systems. Each of these systems was placed in a cubic box of explicit water molecules. A set of five independent simulations (each of 100 ns time scale) was performed for each of these four systems leading to an equilibrium trajectory for each of these systems. Conformations from these equilibrium trajectories were used to estimate the "proximity" of the nitroaromatic compounds to the macrocycles. The criterion for the proximity search was chosen such that the oxygen atom of the phenolic –OH group of PA or the carbon atom of the methyl group of DNT was within a 3 Å radius of any heavy atom (carbon/nitrogen) of the macrocycle. From the calculation, it appears that both PA and DNT spent ~75% of their time in close proximity to the three types of nitrogen atoms of the macrocycles and spent only ~25% of the time in close proximity to the carbon atoms, which proves that the preferential binding modes of the nitroaromatic compounds are ones with the phenolic –OH group of PA or the carbon atom of the methyl group of DNT pointing toward one of the nitrogen atoms of either of the macrocycles. These structures were chosen as the initial configurations for the pulling simulations to estimate the binding free energies of PA and DNT to the macrocycles.

The simulated results showed that picric acid has a preference for N_A over N_B and N_C of both the macrocycles **2** and **3** (for both the macrocycles, N_A and N_B represent the N1 and N4 nitrogen atoms of the pyrazine moiety, respectively; N_C represents the nitrogen atoms of the 3,3′- or 4,4′-bipyridine donor linkers of macrocycles **2** and **3**, respectively). However, this preference for PA is very nominal as the difference of binding energy values between N_A, N_B, and N_C is in the range ~0.03–0.3 kcal/mol in the case of both the macrocycles. So, all three types of nitrogen atoms of macrocycle **2** and **3** behave as competing binding sites for picric acid. But unlike the binding of PA, in the other case, DNT has a higher binding preference for N_B over N_A and N_C of both the macrocycles. The preference is much more prominent due to the difference in the binding free energy values of N_B with respect to N_A and N_C (~0.8–0.9 kcal/mol). However, the same difference is very nominal (~0.03–0.1 kcal/mol) in the case of the rest of the two nitrogen atoms (N_A and N_C), and they act as competing binding sites for DNT.

DOI: 10.1021/acs.inorgchem.5b01156
Inorg. Chem. 2015, 54, 8994–9001

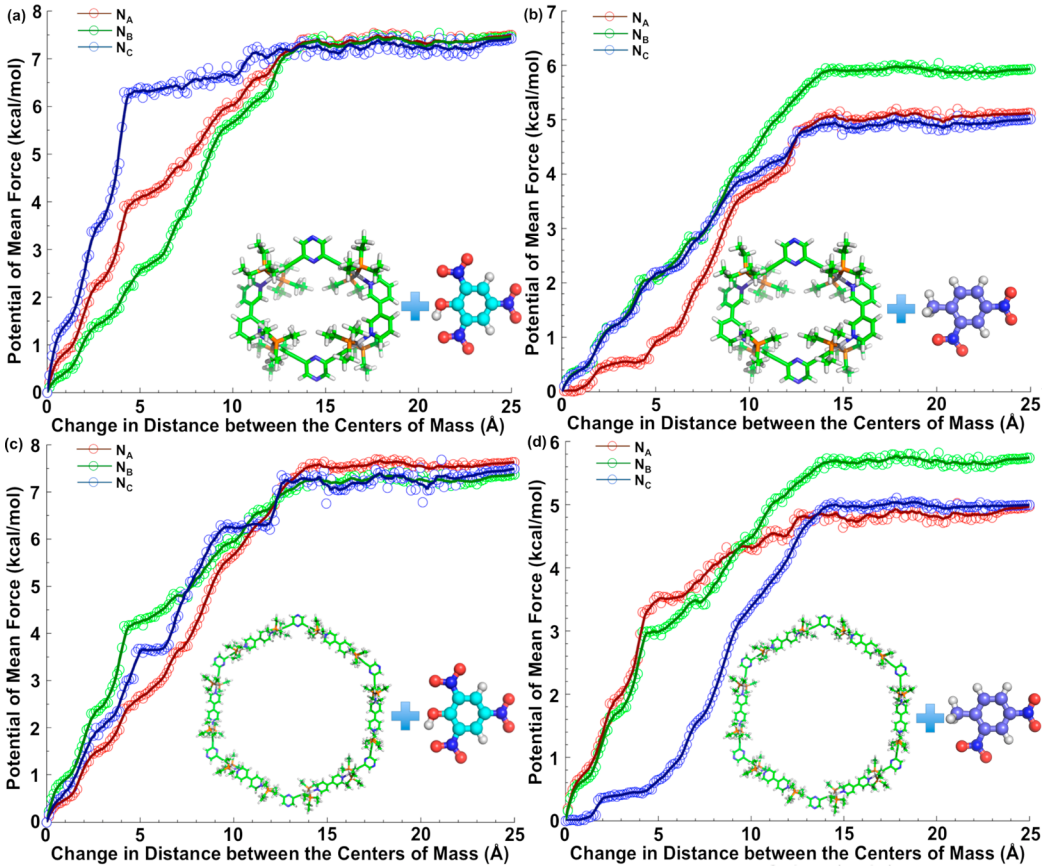

Figure 5. Potential of mean force as a function of the distance between the centers of mass (COMs) of the nitroaromatic compounds (PA and DNT) and the macrocycles (**2** and **3**), (a) macrocycle **2** and PA, (b) macrocycle **2** and DNT, (c) macrocycle **3** and PA, and (d) macrocycle **3** and DNT obtained using umbrella sampling and WHAM. The macrocycles are shown in licorice, and the nitroaromatic compounds are shown in CPK.

The preferable binding propensity of the binding sites of the macrocycles **2** and **3** as obtained by "pulling simulations" toward interaction with both the nitroaromatic guests (PA/DNT) was found to be in good agreement with the conclusions drawn from calorimetric titration experiments (see Figure 5).

CONCLUSION

In conclusion, herein we report the self-assembly of two new cationic molecular hexagons (**2** and **3**) derived from a pyrazine based organometallic acceptor tecton. **2** and **3** are distinctly different from each other with respect to number of supramolecular building blocks involved in their respective self-assembly. Macrocycle **3** is a [6 + 6] self-assembled ensemble, and there are only a handful of examples of such types of supramolecular metallamacrocyles in the literature. However, macrocycle **2** is a unique example of an irregular albeit equiangular and convex molecular hexagon involving a [2 + 2] association of appropriate donor and acceptor tectons. Exclusive formation of these cationic macrocycles (**2** and **3**) has been confirmed by multinuclear (^{1}H and ^{31}P) NMR spectroscopy (including ^{1}H DOSY NMR), ESI-TOF-MS spectrometry, and elemental analyses techniques. Molecular simulation of these macrocycles using the PM6 semiempirical molecular orbital method further ratified their anticipated hexagonal shape. Molecular simulations also indicated these self-assembled ensembles (**2** and **3**) have nanoscalar dimensions. The presence of multiple Pt-ethynyl linkages renders these macrocycles (**2** and **3**) π-electron rich and hence were explored as potential hosts with relatively electron deficient nitroaromatics (DNT = 2,4-dinitrotoluene and PA = picric acid). In this context, using ITC, it can be concluded that these electron-rich macrocycles reported herein have three binding sites (with high binding affinity) to which relatively electron-poor guest molecules (PA and DNT) can bind. Computational simulation studies were performed to obtain insight into preferential binding of the guest molecules among the three binding sites in a given macrocycle. The preferential inclination of the nitroaromatic guests (PA/DNT) for the different three binding sites of the macrocycles (**2** or **3**) was clearly observed in these "pulling simulations" studies. Overall, theoretical simulation results were found to be in good agreement with the conclusions drawn from calorimetric titration experiments. Currently, we are extending this "proof-of-principle" study toward enriching the literature with newer supramolecular frameworks with practical applications in host−guest chemistry, especially for the detection of nitroaromatics.

EXPERIMENTAL SECTION

General Details. All chemicals and anhydrous solvents used in this work were purchased from commercial sources and used without further purification. Linker **1** was prepared by following the protocol reported by Bhowmick et al.[11] FTIR spectra were recorded in a PerkinElmer Spectrum 400 FTIR spectrophotometer. ^{1}H and ^{31}P NMR spectra were recorded on Bruker 400 MHz spectrometers. Elemental analysis was carried out using a Thermo Scientific Flash 2000 organic elemental analyzer. MS analysis was performed on Bruker Impact ESI-Q-TOF system. All the samples were diluted in methanol and infused directly via a standard ESI source using a syringe pump at a flow rate of 180 uL/h. The system was previously calibrated

DOI: 10.1021/acs.inorgchem.5b01156
Inorg. Chem. 2015, 54, 8994−9001

in the mass range of 50−3000 m/z using a tune mix solution. Further data were processed using Data Analysis 4.2 software, while simulated isotope patterns were studied using Bruker Isotope Pattern software. DOSY NMR measurements were performed on a Bruker AV 500 NMR spectrometer using a 5 mm gradient probe at 298 K. DOSY experiments were done with a standard Bruker pulse sequence (ledbpgp2s) with a longitudinal eddy current delay.

General Procedure for the Synthesis of Macrocycles 2 and 3. To the solution of compound **1** (30 mg, 0.024 mmol) in chloroform (5 mL) was added $AgNO_3$ (9 mg, 0.048 mmol) in one portion, and the reaction mixture was stirred for 4 h in the dark at room temperature. The precipitated AgI was filtered off over a bed of Celite, and the filtrate was collected as a pale yellow colored solution. Subsequently, a methanolic solution of the respective bipyridine (0.024 mmol, 0.5 mL) was added dropwise to the aforementioned filtrate with continuous stirring. The reaction mixture was stirred for 10 h at room temperature. Solvents were removed under reduced pressure, and the product obtained was washed several times with diethyl ether to obtain a yellow colored solid that was finally dried in a vacuum. This product was recrystallized as a yellow microcrystalline solid by vapor diffusion of diethyl ether in its corresponding concentrated methanol solution.

Macrocycle **2**. Yield: 30 mg, 85%. ^{1}H NMR (400 MHz, MeOD): δ 9.04 (s, 4H, Ar−H), 8.87−8.86 (d, 4H, J = 4.96 Hz, Ar−H), 8.56−8.53 (d, 4H, J = 8.28 Hz, Ar−H), 8.26 (s, 4H, Ar−H), 7.90−7.86 (m, 4H, Ar−H), 1.88−1.77 (m, 48H, $-CH_2$), 1.16−1.08 (m, 72H, $-CH_3$). ^{31}P{^{1}H} NMR (163 MHz, MeOD): δ 15.25 ($^1J_{PPt}$ = 1131 Hz). FTIR (ATR): 2953, 2880, 2122, 1630, 1490, 1321, 1233, 1145, 1035, 763, 711 cm^{-1}. Anal. calcd for $C_{84}H_{140}N_8P_8Pt_4$: C, 44.05; H, 6.16; N, 4.89. Found: C, 44.12; H, 6.24; N, 4.95. ESI-MS m/z found: $[M-NO_3]^+$ = 2474.76, $[M-2NO_3]^{2+}$ = 1206.39, $[M-3NO_3]^{3+}$ = 783.59, $[M-4NO_3]^{4+}$ = 572.19.

Macrocycle **3**. Yield: 28 mg, 84%. ^{1}H NMR (400 MHz, MeOD): δ 9.03−9.02 (d, 24H, J = 5.84 Hz, Ar−H), 8.33 (s, 12H, Ar−H), 8.29−8.27 (d, 24H, J = 6.2 Hz, Ar−H), 1.96−1.93 (m, 144H, $-CH_2$), 1.30−1.22 (m, 216H, $-CH_3$). ^{31}P{^{1}H} NMR (163 MHz, MeOD): δ 15.78 ($^1J_{PPt}$ = 1135 Hz). FTIR (ATR): 2947, 2886, 2101, 1618, 1482, 1316, 1150, 1029, 802, 742 cm^{-1}. Anal. calcd for $C_{252}H_{420}N_{24}P_{24}Pt_{12}$: C, 44.05; H, 6.16; N, 4.89. Found: C, 44.16; H, 6.25; N, 4.99. ESI-MS m/z found: $[M-4NO_3]^{4+}$ = 1840.58, $[M-6NO_3]^{6+}$ = 1206.39, $[M-8NO_3]^{8+}$ = 889.29, $[M-9NO_3]^{9+}$ = 783.59, $[M-11NO_3]^{11+}$ = 629.21, $[M-12NO_3]^{12+}$ = 572.20.

ITC To Study the Thermodynamics of Host−Guest Chemistry of Macrocycles (2 and 3) and Nitroaromatics. ITC experiments were performed on a MicroCal-iTC200 calorimeter (GE Healthcare Life Science) at 25 °C. All experiments were done using methanol as the solvent. Each experiment was done with 20 consecutive injections (5 mM) of macrocycles (**2** or **3**) into a methanol solution of nitroaromatics (280 μL, 0.5 mM PA, or 0.5 mM DNT) with 2 min intervals between two successive injections. The rotation speed of the syringe was maintained at 600 rpm. The integration of the heat pulses obtained from each titration was fitted using MicroCal Origin 7.0 software to determine the site-binding model corresponding association constant (K).

■ ASSOCIATED CONTENT

Supporting Information

The Supporting Information is available free of charge on the ACS Publications website at DOI: 10.1021/acs.inorgchem.5b01156.

^{1}H and ^{31}P{^{1}H} NMR spectra and ^{1}H DOSY NMR spectra of the metallacycles **2** and **3**, space filling model of metallacycles **2** and **3**, ITC isotherm data and thermodynamic parameters for the binding of metallacycles (**2** and **3**) to nitroaromatics as obtained by ITC, and a detailed simulation protocol (PDF).

■ AUTHOR INFORMATION

Corresponding Author

*E-mail: neeladri@iitp.ac.in or neeladri2002@yahoo.co.in. Tel.: +91 612 2552023. Fax: +91 612 2277383.

Author Contributions

N.D. conceived the research and supervised the work. S.B. synthesized all compounds reported in this manuscript. S.C. performed the ITC experiments and also optimized the energy-minimized geometry of the metallacycles **2** and **3**. S.N. recorded the ESI-TOF mass spectra of the metallacycles **2** and **3**. A.D. carried out the theoretical calculations to study host−guest complexation between macrocycles (**2** and **3**) and nitroaromatics and also optimized the binding free-energy values from "pulling simulations." S.C., A.D., and N.D. wrote and all authors edited the manuscript.

Notes

The authors declare no competing financial interest.

■ ACKNOWLEDGMENTS

N.D. thanks the Indian Institute of Technology (IIT) Patna for financial support. S.B. thanks IIT Patna for an Institute Research Fellowship. The authors also acknowledge Central NMR Facility, CSIR-NCL for DOSY NMR spectra. Prof. Dmitrii E. Makarov is acknowledged for allowing A.D. to use the computational resources at the University of Texas at Austin provided by the Texas Advanced Computing Center. A.D. acknowledges funding from Robert A. Welch foundation (Grant No. F-1514). The authors also acknowledge SAIF-Panjab University for analytical facilities.

■ REFERENCES

(1) (a) Cook, T. R.; Stang, P. J. *Chem. Rev.* **2015**, *115*, 7001. (b) Cook, T. R.; Zheng, Y.-R.; Stang, P. J. *Chem. Rev.* **2013**, *113*, 734. (c) Schoedel, A.; Zaworotko, M. J. *Chem. Sci.* **2014**, *5*, 1269. (d) Tanaka, S.; Tsurugi, H.; Mashima, K. *Coord. Chem. Rev.* **2014**, *265*, 38. (e) Riddell, I. A.; Smulders, M. M. J.; Clegg, J. K.; Hristova, Y. R.; Breiner, B.; Thoburn, J. D.; Nitschke, J. R. *Nat. Chem.* **2012**, *4*, 751. (f) Turega, S.; Whitehead, M.; Hall, B. R.; Haddow, M. F.; Hunter, C. A.; Ward, M. D. *Chem. Commun.* **2012**, *48*, 2752. (g) Bilbeisi, R. A.; Olsen, J. C.; Charbonniere, L. J.; Trabolsi, A. *Inorg. Chim. Acta* **2014**, *417*, 79. (h) Kumar, G.; Gupta, R. *Chem. Soc. Rev.* **2013**, *42*, 9403. (i) Housecroft, C. E. *Dalton Trans.* **2014**, *43*, 6594. (j) Schmidt, A.; Casini, A.; Kuhn, F. E. *Coord. Chem. Rev.* **2014**, *275*, 19. (k) Palma, C. A.; Cecchini, M.; Samori, P. *Chem. Soc. Rev.* **2012**, *41*, 3713. (l) Chakrabarty, R.; Mukherjee, P. S.; Stang, P. J. *Chem. Rev.* **2011**, *111*, 6810. (m) Yan, X.; Cook, T. R.; Wang, P.; Huang, F.; Stang, P. J. *Nat. Chem.* **2015**, *7*, 342. (n) Harris, K.; Fujita, D.; Fujita, M. *Chem. Commun.* **2013**, *49*, 6703.

(2) (a) Chen, L.; Chen, Q.; Wu, M.; Jiang, F.; Hong, M. *Acc. Chem. Res.* **2015**, *48*, 201. (b) Han, M.; Engelhard, D. M.; Clever, G. H. *Chem. Soc. Rev.* **2014**, *43*, 1848. (c) Chakraborty, S.; Mondal, S.; Li, Q.; Das, N. *Tetrahedron Lett.* **2013**, *54*, 1681. (d) Ward, M. D.; Raithby, P. R. *Chem. Soc. Rev.* **2013**, *42*, 1619. (e) Liu, S.; Han, Y.-F.; Jin, G.-X. *Chem. Soc. Rev.* **2007**, *36*, 1543. (f) Galstyan, A.; Sanz Miguel, P. J.; Weise, K.; Lippert, B. *Dalton Trans.* **2013**, *42*, 16151. (g) Alberti, F. M.; Zielinski, W.; Morell Cerda, M.; Sanz Miguel, P. J.; Troeppner, O.; Ivanovic-Burmazovic, I.; Lippert, B. *Chem. - Eur. J.* **2013**, *19*, 9800. (h) Li, Y.; Jiang, Z.; Yuan, J.; Liu, D.; Wu, T.; Moorefield, C. N.; Newkome, G. R.; Wang, P. *Chem. Commun.* **2015**, *51*, 5766. (i) Sarkar, R.; Guo, K.; Moorefield, C. N.; Saunders, M. J.; Wesdemiotis, C.; Newkome, G. R. *Angew. Chem., Int. Ed.* **2014**, *53*, 12182. (j) Ludlow, J. M., III; Tominaga, M.; Chujo, Y.; Schultz, A.; Lu, X.; Xie, T.; Guo, K.; Moorefield, C. N.; Wesdemiotis, C.; Newkome, G. R. *Dalton Trans.* **2014**, *43*, 9604. (k) Saha, M. L.; Neogi, S.; Schmittel, M. *Dalton Trans.* **2014**, *43*, 3815.

DOI: 10.1021/acs.inorgchem.5b01156
Inorg. Chem. 2015, 54, 8994−9001

(3) (a) Han, Y.; Li, J.-R.; Xie, Y.; Guo, G. *Chem. Soc. Rev.* **2014**, *43*, 5952. (b) Li, H.; Han, Y.-F.; Lin, Y. J.; Guo, Z.-W.; Jin, G. X. *J. Am. Chem. Soc.* **2014**, *136*, 2982. (c) Huang, S. L.; Lin, Y. J.; Li, Z. H.; Jin, G. X. *Angew. Chem., Int. Ed.* **2014**, *53*, 11218. (d) Han, Y.; Jia, W.; Yu, W.; Jin, G. *Chem. Soc. Rev.* **2009**, *38*, 3419. (e) Ruben, M.; Rojo, J.; Romero-Salguero, F. J.; Uppadine, L. H.; Lehn, J.-M. *Angew. Chem., Int. Ed.* **2004**, *43*, 3644. (f) Pitt, M. A.; Johnson, D. *Chem. Soc. Rev.* **2007**, *36*, 1441. (g) Perry, J. J., IV; Perman, J. A.; Zaworotko, M. J. *Chem. Soc. Rev.* **2009**, *38*, 1400. (h) Han, Y.-F.; Lin, Y.-J.; Jia, W.-G.; Jin, G.-X. *Organometallics* **2008**, *27*, 4088. (i) Wang, G.-L.; Lin, Y.-J.; Berke, H.; Jin, G.-X. *Inorg. Chem.* **2010**, *49*, 2193. (j) Liu, D.; Ren, Z.-G.; Li, H.-X.; Lang, J.-P.; Li, N.-Y.; Abrahams, B. *Angew. Chem., Int. Ed.* **2010**, *49*, 4767. (k) Zheng, A.-X.; Ren, Z.-G.; Li, L.-L.; Shang, H.; Li, H.-X.; Lang, J.-P. *Dalton Trans.* **2011**, *40*, 589. (l) Sato, S.; Murase, T.; Fujita, M.; Gale, P. A.; Steed, J. W. *Supramolecular Chemistry: From Molecules to Nanomaterials* **2012**, *5*, 2071.

(4) (a) Dydio, P.; Reek, J. N. H. *Chem. Sci.* **2014**, *5*, 2135. (b) Zhang, J.; Biradar, A. V.; Pramanik, S.; Emge, T. J.; Asefa, T.; Li, J. *Chem. Commun.* **2012**, *48*, 6541. (c) Moon, H. R.; Lim, D.-W.; Suh, M. P. *Chem. Soc. Rev.* **2013**, *42*, 1807. (d) Hu, Z.; Deibert, B. J.; Li, J. *Chem. Soc. Rev.* **2014**, *43*, 5815. (e) Mukherjee, P. S.; Pramanik, S.; Shanmugaraju, S. In *Pt/Pd Ethynyl Bond Containing Fluorescent Molecular Architectures As Sensors for Nitroaromatics in Molecular Self Assembly: Advances and Applications*; Li, A. D. Q., Ed.; Pan Stanford Publishing: Singapore, 2013; p 259. (f) Cui, Y.; Yue, Y.; Qian, G.; Chen, B. *Chem. Rev.* **2012**, *112*, 1126. (g) Kreno, L. E.; Leong, K.; Farha, O. K.; Allendorf, M.; Van Duyne, R. P.; Hupp, J. T. *Chem. Rev.* **2012**, *112*, 1105. (h) Liu, B. *J. Mater. Chem.* **2012**, *22*, 10094. (i) Dsouza, N.; Pischel, U.; Nau, W. M. *Chem. Rev.* **2011**, *111*, 7941.

(5) (a) Yoshizawa, M.; Klosterman, J. K. *Chem. Soc. Rev.* **2014**, *43*, 1885. (b) Oliveri, C. G.; Ulmann, P. A.; Wiester, M. J.; Mirkin, C. A. *Acc. Chem. Res.* **2008**, *41*, 1618. (c) Newkome, G. R.; Shreiner, C. *Chem. Rev.* **2010**, *110*, 6338. (d) Stang, P. J.; Olenyuk, B. *Acc. Chem. Res.* **1997**, *30*, 502. (e) Leininger, S.; Olenyuk, B.; Stang, P. J. *Chem. Rev.* **2000**, *100*, 853. (f) Takezawa, Y.; Shionoya, M. *Acc. Chem. Res.* **2012**, *45*, 2066. (g) Fujita, M.; Tominaga, M.; Hori, A.; Therrien, B. *Acc. Chem. Res.* **2005**, *38*, 369. (h) Inokuma, Y.; Kawano, M.; Fujita, M. *Nat. Chem.* **2011**, *3*, 349.

(6) (a) Manna, K.; Zhang, T.; Greene, F. X.; Lin, W. *J. Am. Chem. Soc.* **2015**, *137*, 2665. (b) Lu, K.; He, C.; Lin, W. *J. Am. Chem. Soc.* **2014**, *136*, 16712. (c) Chen, L.-J.; Zhao, G.-Z.; Jiang, B.; Sun; Bin; Wang, M.; Xu, L.; He; Jiuming; Abliz, Z.; Tan, H.; Li, X.; Yang, H.-B. *J. Am. Chem. Soc.* **2014**, *136*, 5993. (d) Kishi, N.; Akita, M.; Kamiya, M.; Hayashi, S.; Hsu, H.-F.; Yoshizawa, M. *J. Am. Chem. Soc.* **2013**, *135*, 12976. (e) Yang, H.-B.; Ghosh, K.; Zhao, Y.; Northrop, B. H.; Lyndon, M. M.; Muddiman, D. C.; White, H. S.; Stang, P. J. *J. Am. Chem. Soc.* **2008**, *130*, 839. (f) Liu, D.; Lu, K.; Poon, C.; Lin, W. *Inorg. Chem.* **2014**, *53*, 1916. (g) Yoon, H. J.; Heo, J.; Mirkin, C. A. *J. Am. Chem. Soc.* **2007**, *129*, 14182. (h) Chen, T.; Pan, G.-B.; Wettach, H.; Fritzsche, M.; Höger, S.; Wan, L.-J.; Yang, H.-B.; Northrop, B. H.; Stang, P. J. *J. Am. Chem. Soc.* **2010**, *132*, 1328.

(7) (a) Xu, L.; Wang, Y.-X.; Chen, L.-J.; Yang, H.-B. *Chem. Soc. Rev.* **2015**, *44*, 2148. (b) Li, Z.-Y.; Zhang, Y.; Zhang, C.-W.; Chen, L.-J.; Wang, C.; Tan, H.; Yu, Y.; Li, X.; Yang, H.-B. *J. Am. Chem. Soc.* **2014**, *136*, 8577. (c) Chan, Y.-T.; Moorefield, C. N.; Soler, M.; Newkome, G. R. *Chem. - Eur. J.* **2010**, *16*, 1768. (d) Perera, S.; Li, X.; Soler, M.; Schultz, A.; Wesdemiotis, C.; Moorefield, C. N.; Newkome, G. R. *Angew. Chem., Int. Ed.* **2010**, *49*, 6539. (e) Chan, Y.-T.; Li, X.; Soler, M.; Wang, J.-L.; Wesdemiotis, C.; Newkome, G. R. *J. Am. Chem. Soc.* **2009**, *131*, 16395. (f) Chen, L.-J.; Li, Q.-J.; He, J.; Tan, H.; Abliz, Z.; Yang, H.-B. *J. Org. Chem.* **2012**, *77*, 1148. (g) Soler, M.; Moorefield, C. N.; Newkome, G. R. *Hexameric Macrocyclic Architectures in Heterocyclic Chemistry*; Advances in Heterocyclic Chemistry; Katritzky, A. R., Ed.; Academic Press: New York, 2010; p 1. (h) Wang, J.-L.; Li, X.; Lu, X.; Chan, Y.-T.; Moorefield, C. D.; Wesdemiotis, C.; Newkome, G. R. *Chem. - Eur. J.* **2011**, *17*, 4830.

(8) (a) Wang, W.; Sun, B.; Wang, X. Q.; Ren, Y. Y.; Chen, L. J.; Ma, J.; Zhang, Y.; Li, X.; Yu, Y.; Tan, H.; Yang, H.-B. *Chem. - Eur. J.* **2015**, *21*, 6286. (b) Wu, N.-W.; Chen, L.-J.; Wang, C.; Ren, Y.-Y.; Li, X.; Xu, L.; Yang, H.-B. *Chem. Commun.* **2014**, *50*, 4231. (c) Wang, W.; Zhang, Y.; Sun, B.; Chen, L.-J.; Xu, X.-D.; Wang, M.; Li, X.; Yu, Y.; Jiang, W.; Yang, H.-B. *Chem. Sci.* **2014**, *5*, 4554. (d) Yang, H.-B.; Das, N.; Huang, F.; Hawkridge, A. M.; Muddiman, D. C.; Stang, P. J. *J. Am. Chem. Soc.* **2006**, *128*, 10014.

(9) (a) Zhang, J.; Marega, R.; Chen, L.-J.; Wu, N.-W.; Xu, X.-D.; Muddiman, D. C.; Bonifazi, D.; Yang, H.-B. *Chem. - Asian J.* **2014**, *9*, 2928. (b) Zhao, L.; Northrop, B. H.; Stang, P. J. *J. Am. Chem. Soc.* **2008**, *130*, 11886. (c) Coronado, E.; Galan-Mascaros, J. R.; Gavina, P.; Marti-Gastaldo, C.; Romero, F. M.; Tatay, S. *Inorg. Chem.* **2008**, *47*, 5197.

(10) (a) Samanta, D.; Mukherjee, P. S. *Dalton Trans.* **2013**, *42*, 16784. (b) Shanmugaraju, S.; Bar, A. K.; Jadhav, H.; Moon, D.; Mukherjee, P. S. *Dalton Trans.* **2013**, *42*, 2998. (c) Chakraborty, S.; Mondal, S.; Bhowmick, S.; Ma, J.; Tan, H.; Neogi, S.; Das, N. *Dalton Trans.* **2014**, *43*, 13270. (d) Chakraborty, S.; Bhowmick, S.; Ma, J.; Tan, H.; Das, N. *Inorg. Chem. Front.* **2015**, *2*, 290. (e) Li, K.; Zou, T.; Chen, Y.; Guan, X.; Che, C.-M. *Chem. - Eur. J.* **2015**, *21*, 7441. (f) Chen, Y.; Che, C.-M.; Lu, W. *Chem. Commun.* **2015**, *51*, 5371. (g) Zhou, F.; Li, S.; Cook, T. R.; He, Z.; Stang, P. J. *Organometallics* **2014**, *33*, 7019. (h) Grishagin, I. V.; Pollock, J. B.; Kushal, S.; Cook, T. R.; Stang, P. J.; Olenyuk, B. Z. *Proc. Natl. Acad. Sci. U. S. A.* **2014**, *111*, 18448.

(11) Bhowmick, S.; Chakraborty, S.; Das, A.; Rajamohanan, P. R.; Das, N. *Inorg. Chem.* **2015**, *54*, 2543.

(12) Stewart, J. J. P. *J. Mol. Model.* **2007**, *13*, 1173.

(13) Schalley, C. A. *Isothermal Titration Calorimetry in Supramolecular Chemistry*; ; Schmidtchen, F. P., Ed.; Wiley-VCH Verlag GmbH & Co. KGaA: Hoboken, NJ, 2012. DOI: 10.1002/9783527644131.

DOI: 10.1021/acs.inorgchem.5b01156
Inorg. Chem. 2015, 54, 8994−9001